Chemical Science

Accepted Manuscript

This article can be cited before page numbers have been issued, to do this please use: X. Lu, G. Zhou, Y. Zeng, Z. Yin, Z. Zhang, L. Guo, Y. Zhai, Y. Yang, H. Wang and L. Li, *Chem. Sci.*, 2019, DOI: 10.1039/C9SC01199D.

ROYAL SOCIETY OF CHEMISTRY

rsc.li/chemical-science

View Article Online
DOI: 10.1039/C9SC01199D

Journal Name

ARTICLE

Single-Step Multivalent Capture Assay for Nucleic Acids Detection with Dual-Affinity Regulation Using Mutation Inhibition and Allosteric Activation

Received 00th January 20xx,
Accepted 00th January 20xx

DOI: 10.1039/x0xx00000x

www.rsc.org/

Xing Lu,‡ Guobao Zhou*,‡ Yanbo Zeng, Zhengzhi Yin, Zulei Zhang, Liping Guo, Yunyun Zhai, Yiwen Yang, Hailong Wang and Lei Li*

The rational modulation of the receptor affinity through distal-site mutation and allosteric control is valuable in biosensor designing to tune the useful dynamic range. Our ability to engineer dual-affinity regulation of receptor refers to diverse affinities of target binding and activities of hybridization chain reaction, however, remains limited. By programmable engineering the switching equilibria of the recognition hairpin using distal-site mutation inhibition and allosteric activation, we obtained a set of receptors varing significantly in affinities of target binding and activities of hybridization chain reaction. For the first time, we developed an electrocatalytic biosensor for nucleic acid detection with tunable dynamic range based on conformational switch triggered bidirectional hybridization chain reaction and blocker assisted multivalent binding. This designable biosensor thus enables single-step incubation, diverse affinities of target binding, diverse efficiencies of signal amplification and diverse single nucleotide discrimination for quantitative analyses of various lengths of nucleic acids in serum, which holds great potential as a compelling platform suitable for liquid biopsy.

Introduction

Mutation and allosteric control are two main strategies for biomolecules regulating their affinities in many naturally occurring biology processes.[1-5] The underlying mechanisms that regulating molecular binding affinities are increasingly providing inspiration in biosensors to tune, extend and narrow the useful detection range. Mutation and allosteric control are often employed in biosensors to regulate diverse affinities of receptors responding to their target molecules, which efficiently transfer a given input to an altered output.[6-10] Biomimetic sensors that employ mutation or allosteric regulation have a broad control of dynamic range, but most of them have low sensitivity of signal transduction.[11,12] The biosensors base on precise valence control of enzyme have high enzymatic amplification for signal transduction. However, they have a limited adjustable dynamic range, which is only depended on the number of linked enzymes.[13,14] The ~~ability to engineer~~ dual-affinity regulation of receptor with diverse affinities of target binding and activities of hybridization chain reaction ideally suits to both extend dynamic range and amplify signal transduction. This unique property of dual-affinity regulation meets the desirable demand of biosensors with tunable dynamic range for the analysis of biomarkers in clinical samples with different concentrations. For example, the levels of overall cell-free DNA expression profile vary from aM level to pM level in peripheral blood samples in both healthy controls and cancer patients.[15,16]

The detection of cell-free DNA expression profiles at the genetic level enables broad liquid biopsy approaches in infection diagnostics,[17] early childhood wheezing[18], fetal chromosome abnormalities[19] and cancer management,[20-25] etc. As cf-DNA is more chemically and bioenvironmentally stable than RNA, cf-DNA is particularly informative, suitable as a molecular biomarker.[26,27] Sensitive, robust and specific detection of DNA plays important role in the efficient diagnosis, prognostic analysis of cancer metastasis and cancer therapies. However, sensitive and single nucleotide resolution detection of DNA remains challenging because of the low abundance of the targets ~~exit~~ in peripheral blood.

In the past decades, ~~there are~~ some popular and potent technologies using signal amplification strategies ~~that~~ have been developed to increase the nucleic acids detection sensitivity. Typically, DNA nanostructure based signal amplification methods mainly include rolling circle reaction (RCA),[28-34] hybridization chain reaction (HCR),[35-44] entropy-driven catalysis (EDC)[45-48] and catalyzed hairpin assembly (CHA),[49-54] etc. Hybridization chain reaction is even widely employed in biosensors to amplify signal. Fan and coworkers had integrated the hybridization chain reaction amplification and tetrahedral DNA nanostructure (with outstanding hybridization condition) to build ultrasensitive nucleic acids

College of Biological, Chemical Sciences and Engineering, Jiaxing University, Jiaxing 314001, China. Email: lei.li@mail.zjxu.edu.cn, gbzhou@mail.zjxu.edu.cn
†Electronic Supplementary Information (ESI) available: Experimental procedures, table of detailed DNA sequences and supporting figures. See DOI: 10.1039/x0xx00000x
‡ These authors contributed equally.

View Article Online
DOI: 10.1039/C9SC01199D

detection platform.[38] However, it suffers from extensively sample processing with multiple steps of incubations and washes, which restrain their applications in on-site, real time analytical devices suitable for point of care (POC) detection.

Existing hybridization chain reaction amplified biosensors have several disadvantages. First, the efficiency of hybridization chain reaction occurred on interface is low due to the limited mass transfer of the hairpins to the surface. Second, the hairpin probes used in hybridization chain reaction are not universal due to the sequences of the hairpins varied with the change of initiator sequence. Third, the stabilities of the hairpins that will affect the signal to noise (S/N) ratio are greatly depended on the target sequence. Fourth, although ultrasensitive nucleic acids detection performance has been obtained by using hybridization chain reaction amplification, multiple processing steps are always required. The cancer cell capture and analysis employing multibranched hybridization chain reaction proposed by Zuo and coworkers[55] had solved some of above problems. However, the excess unreacted hairpins incubated with cancer cells should be removed by several centrifugation and washing steps. These processes will lead to serious loss of cancer cells. In this work, excess unreacted hairpins can't be separated easily from target induced multibranched hybridization chain reaction products. So we proposed the blocker assisted multivalent capture strategy to prohibit the excess hairpins competitive binding with capture probes on surface (Fig. 1, bottom).

Here, we verified the utility of varying the switching equilibrium constant of the receptor to modulate both target binding affinity and hybridization chain reaction activity. The useful detection range of the constructed electrocatalytic biosensor was regulated through distal-site mutation inhibition and allosteric activation (Fig. 1, top). The dual-affinity regulation applied in our biosensor not only obtained a broad dynamic range but also amplified the signal transduction. In addition, we re-engineered the traditional toehold initiated hybridization chain reaction to conformational switch induced multibranched and bidirectional hybridization chain reaction (mbHCR), which can produce long chain products with multiple branched arms for multivalent capture and multiple biotins linked with SA-HRP for further signal amplification. Blocker was employed to prevent the binding of unreacted hairpins with probes on electrode. Thus, the target binding, signal amplification, and multivalent binding can be finished in single-step incubation. Furthermore, by employing the allosteric activation strategy, we could sensitively detect diverse lengths of nucleic acids with excellent selectivity using the universal signal reporter in diluted serum.

Results and discussion

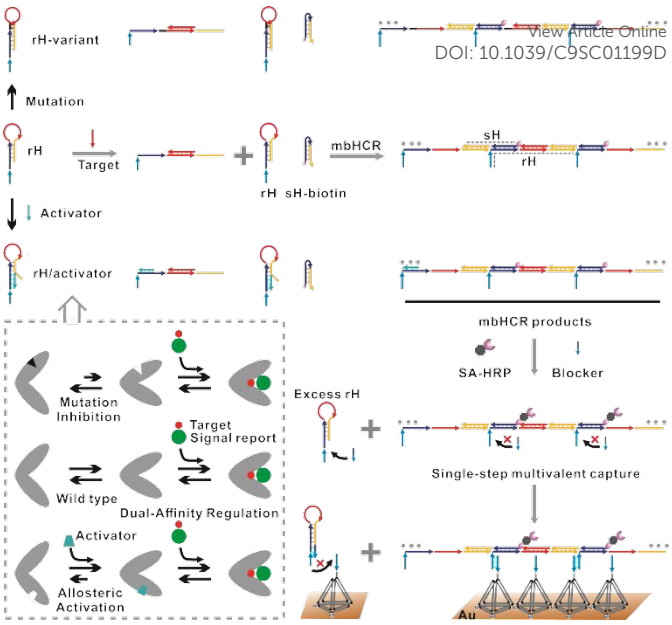

Fig. 1 Top, dual-affinity regulation through distal-site mutation inhibition and allosteric activation was designed here to tune target binding affinity and hybridization chain reaction activity. Bottom, schematic of blocker assisted single-step electrocatalytic assay for nucleic acid detection based on conformational switch induced multibranched and bidirectional hybridization chain reaction. First, the binding of target to rH initiated hybridization chain reaction along both directions. HCR products were then pretreated with SA-HRP and blocker. Blocker was used to prevent competitive capture of unreacted rH.

The design of the single-step electrocatalytic assay for analysis of nucleic acids is depicted in Fig. 1. Our re-engineered multibranched and bidirectional hybridization chain reaction contains two monomer hairpins: recognition hairpin (rH) with a single-stranded extension at the 5'termination and signal hairpin (sH-biotin). The sequences of two hairpins used in this work are followed the sequences designed by Pierce and coworkers[56] except a section of sequence was inserted in the rH for target recognition. In the absence of target, the rH and sH do not hybridize each other due to the hairpins are protected by long stems, and therefore the ~~suppressing~~ signal output is suppressed. Binding of a specific target DNA sequence to the loop of rH breaks the stem and triggers hybridization chain reaction at both directions by the two hairpins into mutlibranched ~~nicked~~ double helix. The long mbHCR products are produced for the efficient electrochemical signal amplification and the multivalent capture. In order to obtain target binding, hybridization chain reaction and multivalent capture at single-step incubation, the mbHCR products are pretreated with SA-HRP and blocker. With optimized design, the blocker is employed to hybridize with unreacted rH and thereby it helps to prevent the capture of excess rH on the gold electrode surface. However, the blocker can not hybridize easily with the rH in mbHCR products due to the low equilibrium stability. It is important to note that the adding of active-2 for enhancing rH binding affinity will not

View Article Online
DOI: 10.1039/C9SC01199D

disrupt the hybridization of rH with blocker. This assumption was estimated via NUPACK at 25°C (Fig. S1).

The useful dynamic range of the DNA binding switch and hybridization chain reaction are controlled by using distal-site mutation inhibition and allosteric activation, in which target binding affinity and hybridization chain reaction activity are controlled by either destabilize or stabilize the receptor (Fig. 1B). To create this situation, we tuned the switching equilibria of rH to alter its dual-affinity by reducing or extending the length of stem in rH. The free energies of rH were estimated via NUPACK at 25°C (Fig. S2). It ~~is~~ decreased from -26.07 kcal/mol (rH, original hairpin with 18 base pairs of stem) to -30.63 kcal/mol (rH-v1, 21 base pairs of stem) and -35.41 kcal/mol (rH-v2, 24 base pairs of stem) indicating the progressively reducing the dual-affinity of the receptors through mutation inhibition. When adding allosteric effector activator 1 or activator 2 (see sequences listed in Table S1) to help opening the hairpin structure, the equilibrium probability of stem in rH decreased suggesting the easier opening of rH-a1 and rH-a2 by target DNA than that of original rH.

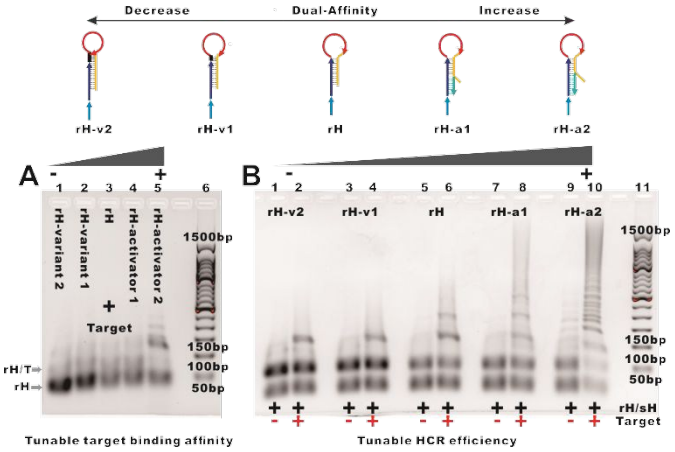

Fig. 2 (A) Analysis by AGE of reactions of receptors with target. Lane 1, 1 μM rH-v2+ 0.2 μM target-24; Lane 2, 1 μM rH-v1 + 0.2 μM target-24; Lane 3, 1 μM rH + 0.2 μM target-24; Lane 4, 1 μM rH-a1 + 0.2 μM target-24; Lane 5, 1 μM rH-a2 + 0.2 μM target-24; Lane6, 50bp DNA ladder markers. (B) Analysis by AGE of the mutation inhibition and allosteric activation controlled multibranched hybridization chain reaction. Lane 1, 1 μM rH-v2/sH. Lane 2, 1 μM rH-v2/sH and 0.2 μM target-24. Lane 3, 1 μM rH-v1/sH. Lane 4, 1 μM rH-v1/sH and 0.2 μM target-24. Lane 5, 1 μM rH/sH. Lane 6, 1 μM rH/sH and 0.2 μM target-24. Lane 7, 1 μM rH-a1/sH. Lane 8, 1 μM rH-a1/sH and 0.2 μM target-24. Lane 9, 1 μM rH-a2/sH. Lane 10, 1 μM rH-a2/sH and 0.2 μM target-24. Lane 11, 50bp DNA ladder markers.

To demonstrate the feasibility of tuning the target binding affinity and hybridization chain reaction activity of mbHCR, gel electrophoresis analysis was first investigated. The product of receptor hybridized with target increased with the reduced switching equilibrium constant of rH (Fig. 2A). The product of mbHCR was also apparently related to the stability of rH. The molecular weight of mutlibranched nicked double helix became larger by decreasing the stability of the rH (Fig. 2B), which demonstrated the negative and positive modulating the target binding affinity and hybridization chain reaction activity though mutation inhibition and allosteric activation.

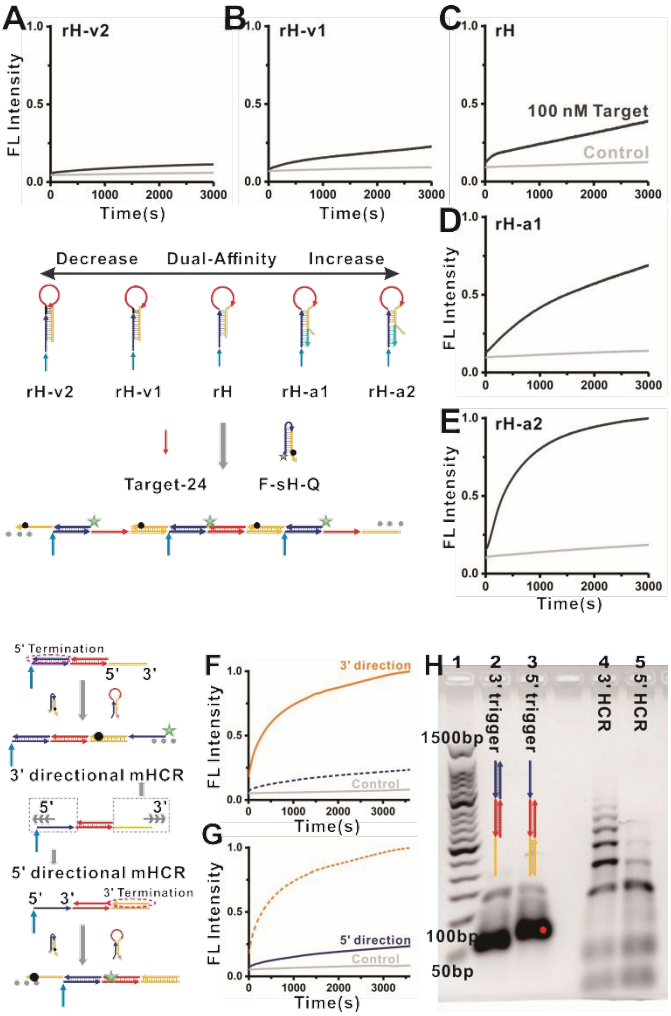

Fig. 3 Kinetics of mbHCR with dual-affinity regulation. 0 or 100 nM target-24 was added into the system at t≈0. Fluorescence intensity of each sample was monitored within 10 s after mixing by pipetting. Here, [rH] = [F-sH-Q] = 50 nM. The control trace (light gray) and reaction trace (green) show the mbHCR was initiated with 0 or 100 nM target-24. The kinetic of mbHCR was hindered by mutation inhibition (A, B) or accelerated by adding allosteric effectors (D, E). (F, G) Kinetics of hybridization chain reaction initiated along two directions. Same amount of 3'trigger (F) or 5'trigger (G) was added into the system at t≈0. Increasing traces of fluorescence indicated the loop-toehold initiated hybridization chain reaction is slower than the end-toehold initiated hybridization chain reaction. (H) Analysis by AGE of the two directional hybridization chain reactions. lane 1, 50bp DNA ladder markers; Lane 2, 3 μM 3'trigger (3 μM rH + 3 μM target-24 + 3 μM 5'termination); lane 3, 3 μM 5'trigger (3 μM rH + 3 μM target-24 + 3 μM 3'termination); lane 4, 3'mbHCR (1 μM rH + 1 μM sH-biotin + 0.2 μM 3'trigger); lane 5, 5'mbHCR(1 μM rH + 1 μM sH-biotin + 0.2 μM 5'trigger).

We next characterized the kinetics of the dual-affinity controlled mbHCR through monitoring the fluorescence intensity change initiated by 0 or 100 nM target DNA. By employing mutation inhibition and allosteric activation to

View Article Online DOI: 10.1039/C9SC01100D

modulate the target binding affinity and hybridization chain reaction activity of the receptors, the kinetic rate of fluorescence intensity increased with the increasement of dual-affinity (Fig. 3A-E). We further demonstrated the bidirectional initiation of mbHCR in the following experiments. 5'termination (obtain 3'trigger) and 3'termination (obtain 5'trigger) were employed to block one direction initiator. Then we monitored the real time fluorescence intensity of hybridization chain reaction induced by same amount of 3'trigger and 5'trigger (Fig. 3F and 3G). We observed a relatively low rate constant for 5'directional HCR due to the loop-based displacement in 5'directional HCR was harder (much higher energy barrier to open hairpin) than the toehold-based displacement in 3'directional HCR. The AGE analysis further proved the lower efficiency of 5'directional HCR than 3'directional HCR (Fig. 3H).

Having validated the facile dual-affinity regulation of mbHCR, we next attempted to detect nucleic acid through electrochemical way. Our previous work have proved the multivalent hybridization capture efficiency on surface is higher than monomer hybridization.[55] However, a limitation existing here is that the unreacted monomer hairpin can't be removed easily from mbHCR products. In order to obtain the DNA analysis completed at single-step incubation and wash, we first employed the gap hybridization strategy[57] to diminish the binding efficiency of monomer hybridization on surface. The monomer hybridization is destabilized because a 10-nt gap is reserved between the capture probe and rH stem. Tetrahedron DNA nanostructures (Fig. S3 validated the successfully self-assembly of TDN) with capturing probe on vertex were employed to capture the target induced mbHCR products and generate the electrocatalytic i-t current of the enzymatic reaction. We investigated the influence of the capture reaction temperature and the length of single-stranded extension in rH. We found that the reactions were taking place well at 37°C (Fig. S4). Under the optimal incubation temperature, the S/N was enhanced with the increased length of single-stranded extension in rH (Fig. S5). However, the influence of 10-nt gap generated instability of hybridization will be weakened by increasing the extension length of rH, which means the competitive hybridization of excess rH with capture probe will dramatically disrupt the detection of target nucleic acid at the low concentrations. The sensitivity of target-24 analysis using rH-Target-24(4-10) was better than that using rH-Target-24(4-12) (data not shown).

To settle above limitations, we then employed the blocker to hybridize prior with excess rH prohibiting its capture on surface. The hybridization cases of diverse lengths of blocker with mbHCR product and rH were estimated via NUPACK at 25°C (Fig. S6, Fig. S7). The hybridization probabilities of blocker with mbHCR product and rH are both enhanced with the increased length of blocker (Fig. 4, top). The detection performance influenced by the length of blocker was then investigated. We found that 12-nt of blocker was optimized to produce the best S/N (Fig. 4, bottom). This is because the 14-nt blocker binding to mbHCR products with high efficiency will prevent the multivalent capture. The 10-nt blocker has the lowest probability binding to mbHCR product. However, the 10-nt extension in rH-Target-24(4-6) has relative lower efficiency of multivalent capture when compared with 12-nt extension in rH-Target-24(6-6). The results also show that the background signal produced at 25°C was lower than that produced at 37°C (37°C used in Fig. S5 and 25°C used in Fig. 4).

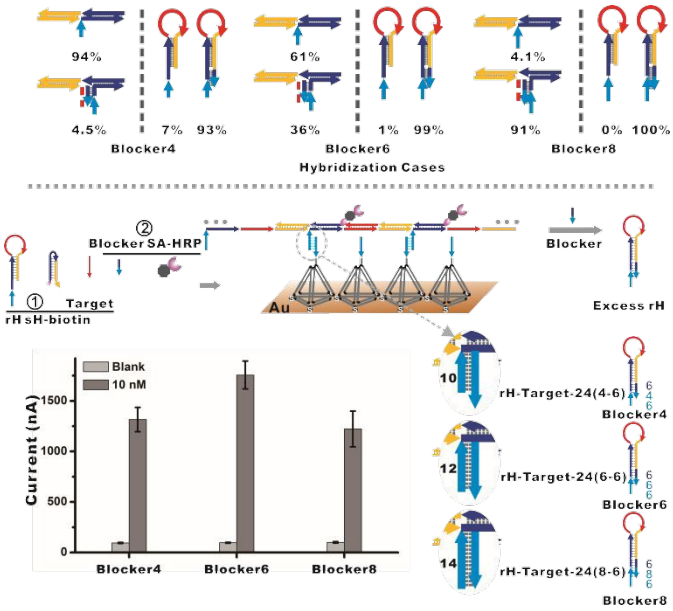

Fig. 4 (Top) Hybridization cases of diverse lengths of blocker with mbHCR product and rH were estimated via NUPACK. The percentages were calculated from Fig. S6 and Fig. S7. (Bottom) Blocker was employed to hybridize prior with excess rH, which will prohibit the hybridization of rH with capture probe on surface. The length of blocker influenced in detection performance was investigated.

Our previous work ~~had~~ also demonstrated that the multivalent capture obtained nearly saturated hybridization efficiency in 15 minutes at room temperature.[55] Multivalent binding reaction was carried out within 30 minutes in this work. As predicted, when we used the five rH with different target binding affinities and hybridization chain reaction activities for nucleic acids analysis, the detection limits shifted in intervals by almost one order of magnitude. With the increasing in the dual-affinity of rH, the detection limit was enhanced from 5 nM (rH-v2) to 10 fM (rH-a2) (Fig. 5). With this rational regulation, the detection sensitivity could be tuned about 500000-fold. Hybridization chain reaction performed in solution and the multivalent capture performed on surface are both efficient. Thus the nucleic acid analysis performances (detection sensitivity and detection speed) are outstanding (Table S2). Further optimization (such as optimize the concentration of activator) can probably lead to even higher sensitivity.

View Article Online
DOI: 10.1039/C9SC01109D

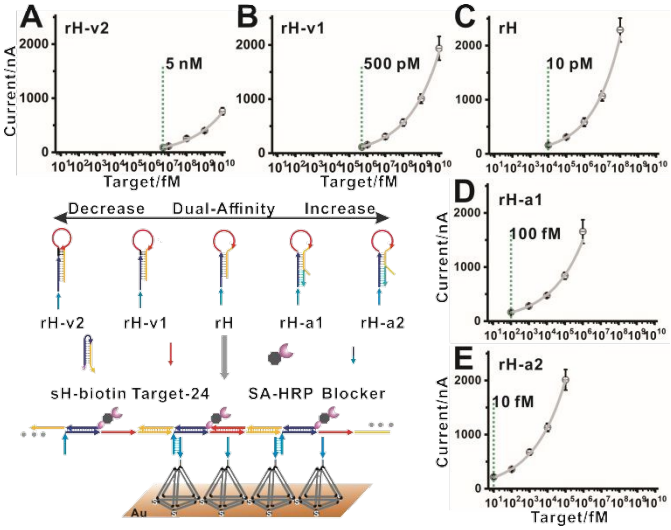

Fig. 5 Blocker assisted single-step electrocatalytic assay. The detection limits were 5 nM, 500 pM, 10 pM, 100 fM, 10 fM for (A) rH-v2, (B) rH-v1, (C) rH, and (D) rH-a1, (E) rH-a2, respectively.

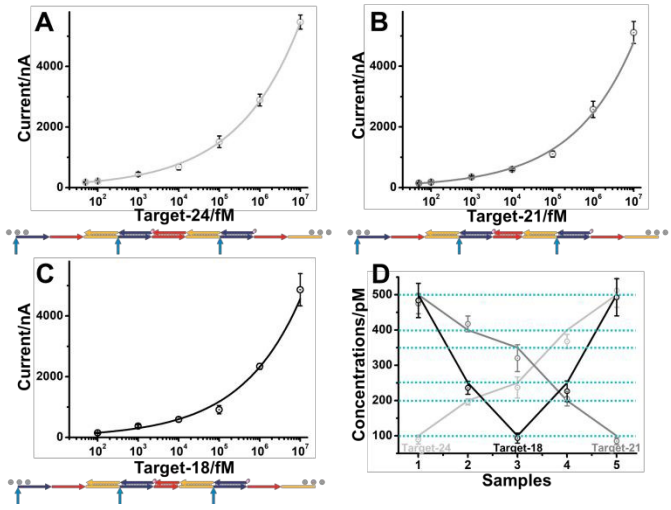

Fig. 6 Analysis of diverse lengths of nucleic acids in 75% serum and 25% of 2× SPSC buffer. Logarithmic plot of amperometric current versus target-24 (A) (light gray), target-21 (B) (gray) and target-18 (C) (black) concentrations using electrocatalytic mbHCR strategy. (D) Five samples (1 to 5) containing varying amounts of target-24 (light gray), target-21 (gray) and target-18 (black) (lines indicate the known concentrations) were measured. Results deviated from the lines are due to experimental errors.

The constructed single-step electrocatalytic assay using rH-a2 with high sensitivity could also be adapted for analysis of diverse lengths of nucleic acids in diluted serum. The detection performance in serum with or without dilution is shown in Fig. S8. We obtained an optimized S/N in 75% serum and 25% of 2× SPSC buffer. The reduced signal observed in serum is possibly due to the added biomolecules nonspecific interaction with target DNA and the decrease of salt concentration in serum, which will decrease the efficiency of target binding and hybridization chain reaction. The sequences of signal hairpin could be kept in same benefiting from the recognition site designed here is at the loop of the recognition hairpin, thus the signal hairpin could be universally used in different nucleic acids detection. Fig. 6A–C show the excellent performance for the analysis of the three diverse lengths of DNA targets with detection limits of 50 fM (target-DNA-24), 50 fM (target-DNA-21), and 100 fM (target-DNA-18), respectively. The AGE analysis, typical CV curves and i-t curves all validated the mbHCR triggered by target-DNA-18 was less efficient than that triggered by target-DNA-24 and target-DNA-21 (Fig. S9-Fig. S11). Five samples (S1 to S5) containing different amounts of nucleic acids (lines indicate the known concentrations) were measured. The results (Fig. 6D) show an impressive validation of the well accurate of our single-step electrocatalytic assay in 75% serum and 25% of 2× SPSC buffer.

The sequence-specificity of our assay with single mismatch targets in various locations was considered at last. Clearly, perfectly matched target could be easily differentiated from other mismatches at the same concentration of 10 nM in buffer by using rH-a2 as receptor, revealing a good single nucleotide resolution (Fig. S12). The location of single-base mismatch did not affect significantly in signal output. It is easy to distinguish a perfectly matched target from five single-base mismatch of target at different locations (Fig. S13). Besides, the selectivity can be increased by using rH-v2 as receptor due to higher energy barrier has to be broken to open the recognition hairpin (Fig. S14). These results successfully demonstrate the high potential of the electrocatalytic assay as a single nucleotide resolution biosensor for nucleic acids detection in clinical samples.

Conclusions

In summary, a novel single-step electrocatalytic strategy, called blocker assisted mbHCR, has been proposed. This method enables the detection of nucleic acid with tunable detection range by programmable modulating the target binding affinity and hybridization chain reaction activity using mutation inhibition and allosteric activation. The dual-affinity regulation demonstrated here both extended the dynamic range and amplified the signal transduction. Blocker assisted single-step strategy and dual-affinity regulation can be applied in other solid-phase biosensors. Besides, the detection cost can be reduced as the signal hairpin is universal. The selectivity of single nucleotide polymorphism also can be tuned through dual-affinity regulation. The analysis of multiple lengths of DNA in serum with high precision revealed the high potential of the constructed strategy as a reliable and sensitive electrocatalytic biosensor for the detection of nucleic acids in complex matrices.

Conflicts of interest

There are no conflicts to declare.

View Article Online
DOI: 10.1039/C9SC01199D

Acknowledgements

This work was supported by the National Natural Science Foundation of China (NSFC Grants 21677060 and 21507041), the Zhejiang Provincial Natural Science Foundation of China (Grants LQ19B050002, LY16B050007 and Y18B050014).

Notes and references

1 V. J. Hilser, J. O. Wrabl and H. N. Motlagh, *Annu. Rev. Biophys.*, 2012, **41**, 585-609.
2 A. del Sol, C.-J. Tsai, B. Ma and R. Nussinov, *Structure*, 2009, **17**, 1042-1050.
3 S. A. Benner, *Chem. Rev.*, 1989, **89**, 789-806.
4 C. J. Tsai, A. del Sol and R. Nussinov, *Mol. BioSyst.*, 2009, **5**, 207-216.
5 C. Y. Huang and J. E. Ferrell, *P. Natl. Acad. Sci. USA.*, 1996, **93**, 10078-10083.
6 A. J. Simon, A. Vallee-Belisle, F. Ricci and K. W. Plaxco, *P. Natl. Acad. Sci. USA.*, 2014, **111**, 15048-15053.
7 J. S. Marvin, E. E. Corcoran, N. A. Hattangadi, J. V. Zhang, S. A. Gere and H. W. Hellinga, *P. Natl. Acad. Sci. USA.*, 1997, **94**, 4366-4371.
8 J. L. Vinkenborg, N. Karnowski and M. Famulok, *Nat. Chem Biol.*, 2011, **7**, 519-527.
9 Y. Xiang, A. Tong and Y. Lu, *J. Am. Chem. Soc.*, 2009, **131**, 15352-15357.
10 F. Ricci, A. Vallee-Belisle, A. Porchetta and K. W. Plaxco, *J. Am. Chem. Soc.*, 2012, **134**, 15177-15180.
11 A. Vallee-Belisle, F. Ricci and K. W. Plaxco, *J. Am. Chem. Soc.*, 2012, **134**, 2876-2879
12 A. Porchetta, A. Vallee-Belisle, K. W. Plaxco and F. Ricci, *J. Am. Chem. Soc.*, 2012, **134**, 20601-20604.
13 Y. L. Xianyu, J. Wu, Y. P. Chen, W. S. Zheng, M. X. Xie and X. Y. Jiang, *Angew. Chem. Int. Ed.*, 2018, **57**, 7503-7507.
14 Q. Liu, Z. L. Ge, X. H. Mao, G. B. Zhou, X. L. Zuo, J. W. Shen, J. Y. Shi, J. Li, L. H. Wang, X. Q. Chen and C.H. Fan, *Angew. Chem. Int. Ed.*, 2018, **57**, 7131-7135.
15 L. Cabel, C. Proudhon, E. Romano, N. Girard, O. Lantz, M. H. Stern, J. Y. Pierga and F. C. Bidard, *Nat. Rev. Clin. Oncol.*, 2018, **15**, 639-650.
16 J. Das, I. Ivanov, L. Montermini, J. Rak, E. H. Sargent and S. O. Kelley, *Nat. Chem.*, 2015, **7**, 569-575.
17 N. R. Y. Ho, G. S. Lim, N. R. Sundah, D. Lim, T. P. Loh and H. Shao, *Nat. Commun.*, 2018, **9**, 3238.
18 B. A. Turturice, D. R. Gold, A. A. Litonjua, E. Oken, S. Rifas-Shiman, D. L. Perkins and P. W. Finn, *J. Allergy, Clin. Immun*., 2018, 10.1016/j.jaci.2018.06.051.
19 D. W. Bianchi and R. W. K. Chiu, *New. Engl. J. Med.*, 2018, **379**, 464-473.
20 L. D. Mattos-Arruda, B. Weigelt, J. Cortes, H. H. Won, C. K. Y. Ng, P. Nuciforo, F. C. Bidard, C. Aura, C. Saura, V. Peg, S. Piscuoglio, M. Oliveira, Y. Smolders, P. Patel, L. Norton, J. Tabernero, M. F. Berger, J. Seoane and J. S. Reis-Filho, *Ann. Oncol.* 2018, **25**, 1729-1735.
21 W. K. J. Lam, P. Jiang, K. C. A. Chan, S. H. Cheng, H. Zhang, W. Peng, O. Y. O. Tse, Y. K. Tong, W. Gai, B. C. Y. Zee, B. B. Y. Ma, E. P. Hui, A. T. C. Chan, J. K. S. Woo, R. W. K. Chiu and Y. M. D. Lo, *P. Natl. Acad. Sci. USA*, 2018, **115**, E5115-E5124.
22 P. Hu, S. Zhang, T. Wu, D. Ni, W. Fan, Y. Zhu, R. Qian and J. Shi, *Adv. Mater.*, 2018, **30**, 1801690.
23 L. Cabel, C. Proudhon, E. Romano, N. Girard, O. Lantz, M.-H. Stern, J. Y. Pierga and F. C. Bidard, *Nat. Rev. Clin. Oncol.*, 2018. **15**, 639-650.
24 A. M. Newman, A. F. Lovejoy, D. M. Klass, D. M. Kurtz, J. J. Chabon, F. Scherer, H. Stehr, C. L. Liu, S. V. Bratman, C. Say, L. Zhou, J. N. Carter, R. B. West, G. W. Sledge Jr, J. B. Shrager, B. W. Loo Jr, J. W. Neal, H. A. Wakelee, M. Diehn and A. A. Alizadeh, *Nat. Biotech.*, 2016, **34**, 547-555.
25 S.-J. Dawson, D. W. Y. Tsui, M. Murtaza, H. Biggs, O. M. Rueda, S.-F. Chin, M. J. Dunning, D. Gale, T. Forshew, B. Mahler-Araujo, S. Rajan, S. Humphray, J. Becq, D. Halsall, M. Wallis, D. Bentley, C. Caldas and N. Rosenfeld, *New. Engl. J. Med.*, 2013, **368**, 1199-1209.
26 J. Das, I. Ivanov, E. H. Sargent and S. O. Kelley, *J. Am. Chem. Soc.*, 2016, **138**, 11009-11016.
27 S. K. Silverman, *Acc. Chem. Res.*, 2009, **42**, 1521-1531.
28 X. Li, X. W. Xu, J. Song, Q. W. Xue, C. Z. Li and W. Jiang, *Biosens. Bioelectron*, 2017, **91**, 631-636.
29 Y. Q. Chen, Y. Y. Song, F. Wu, W. T. Liu, B. S. Fu, B. K. Feng and X. Zhou, *Chem. Commun.*, 2015, **51**, 6980-6983.
30 J. Hu, M. H. Liu and C. Y. Zhang, *Chem. Sci.*, 2018, **9**, 4258-4267.
31 L. Tang, Y. Liu, M. M. Ali, D. K. Kang, W. Zhao and J. H. Li, *Anal. Chem.*, 2012, **84**, 4711-4717.
32 R. Deng, L. Tang, Q. Tian, Y. Wang, L. Lin and J. H. Li, *Angew. Chem. Int. Ed.*, 2014, **126**, 2421-2425.
33 R. Deng, K. Zhang and J. H. Li, *Acc. Chem. Res.*, 2017, **50**, 1059-1068.
34 X. Tang, R. Deng, Y. Sun, X. Ren, M. Zhou and J. H. Li, *Anal. Chem.*, 2018, **90**, 10001-10008.
35 J. Huang, H. Wang, X. Yang, K. Quan, Y. Yang, L. Ying, N. Xie, M. Ou and K. M. Wang, *Chem. Sci.*, 2016, **7**, 3829-3835.
36 J. Huang, Y. Wu, Y. Chen, Z. Zhu, X. Yang, C. J. Yang, K. M. Wang and W. H. Tan, *Angew. Chem. Int. Ed.*, 2011, **50**, 401-404.
37 M. Ou, J. Huang, X. Yang, X. He, K. Quan, Y. Yang, N. Xie, J. Li and K. M. Wang, *ChemBioChem.*, 2018, **19**, 147-152.
38 Z. L. Ge, M. H. Lin, P. Wang, H. Pei, J. Yan, J. Y. Sho, Q. Huang, D. N. He, C. H. Fan and X. L. Zuo, *Anal. Chem.*, 2014, **86**, 2124-2130.
39 H. M. T. Choi, V. A. Beck and N. A. Pierce, *ACS. Nano.*, 2014, **8**, 4284-4294.
40 S. Bi, S. Yue and S. Zhang, *Chem. Soc. Rev.*, 2017, **46**, 4281-4298.
41 Z. Wu, G. Q. Liu, X. L. Yang and J. H. Jiang, *J. Am. Chem. Soc.*, 2015, **137**, 6829-6836.
42 J. Wei, X. Gong, Q. Wang, M. Pan, X. Liu, J. Liu, F. Xia and F. Wang, *Chem. Sci.*, 2018, **9**, 52-61.
43 F. Wang, J. Elbaz, R. Orbach, N. Magen and I. Willner, *J. Am. Chem. Soc.*, 2011, **133**, 17149-17151.
44 P. Liu, X. Yang, S. Sun, Q. Wang, K. M. Wang, J. Huang, J. Liu and L. He, *Anal. Chem.*, 2013, **85**, 7689-7695.
45 Y. Wang, L. Tang, Z. Li, Y. Lin and J. H. Li, *Nat. Protoc.*, 2014, **9**, 1944.
46 C. P. Liang, P. Q. Ma, H. Liu, X. Guo, B. C. Yin and B. C. Ye, *Angew. Chem. Int. Ed.*, 2017, **56**, 9077-9081.
47 D. Y. Zhang, A. J. Turberfield, B. Yurke and E. Winfree, *Science*, 2007, **318**, 1121-1125.
48 Y. Lv, L. Cui, R. Peng, Z. Zhao, L. Qiu, H. Chen, C. Jin, X. B. Zhang and W. H. Tan, *Anal. Chem.*, 2015, **87**, 11714-11720.
49 Q. Wei, J. Huang, J. Li, J. Wang, X. Yang, J. Liu and K. M. Wang, *Chem. Sci.*, 2018, **9**, 7802-7808.
50 K. Quan, J. Huang, X. Yang, Y. Yang, L. Ying, H. Wang, N. Xie, M. Ou and K. M. Wang, *Anal. Chem.*, 2016, **88**, 5857-5864.
51 C. Wu, S. Cansiz, L. Zhang, I. T. Teng, L. Qiu, J. Li, Y. Liu, C. Zhou, R. Hu, T. Zhang, C. Cui, L. Cui and W. Tan, *J. Am. Chem. Soc.*, 2015, **137**, 4900-4903.
52 R. Deng, K. Zhang, Y. Sun, X. Ren and J. H. Li, *Chem. Sci.*, 2017, **8**, 3668-3675.
53 C. Jung, P. B. Allen and A. D. Ellington, *Nat. Nano.*, 2015, **11**, 157.
54 J. Liu, P. Du, J. Zhang, H. Shen and J. Lei, *Chem. Commun.*, 2018, **54**, 2550-2553.

View Article Online
DOI: 10.1039/C9SC01199D

55 G. B. Zhou, M. H. Lin, P. Song, X. Q. Chen, J. Chao, L. H. Wang, Q. Huang, W. Huang, C. H. Fan and X. L. Zuo, *Anal. Chem.*, 2014, **86**, 7843-7848.
56 R. M. Dirks and N. A. Pierce, *P. Natl. Acad. Sci. USA.*, 2004, **101**, 15275-15278.
57 C. Poehlmann, M. Sprinzl, *Anal. Chem.* 2010, **82**, 4434-4440.

Table of contents entry

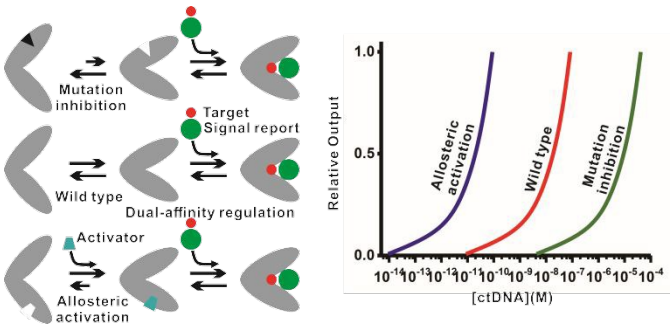

The single-step electrocatalytic biosensor with dual-affinity regulation enables tunable dynamic range and tunable single nucleotide resolution for nucleic acid detection.